Supporting Information

$Cu_3Mo_2O_9/BiVO_4$ heterojunction film with integrated thermodynamic and kinetic advantages for solar water oxidation

Biao Xiong, [†] Yuting Wu, [†] Jinyan Du, [†] Jie Li, [†] Binyao Liu, [†] Gaili Ke, [†] Huichao He, [†*] Yong Zhou [‡ *]

[†]State Key Laboratory of Environmental-Friendly Energy Materials, School of Materials Science and Engineering, Southwest University of Science and Technology, Mianyang 621010, China.

[‡]Ecomaterials and Renewable Energy Research Center, School of Physics, Nanjing University, Nanjing 211102, China.

Huichao He: E-mail: hehuichao@swust.edu.cn;

Yong Zhou: E-mail: zhouyong1999@nju.edu.cn;

Number of pages: 16

Number of figures: 10

Number of tables: 1

1. EXPERIMENTAL SECTION

1.1 Preparation of $BiVO_4$ film

The $BiVO_4$ film was prepared on fluorine-doped tin oxide glass substrate (FTO, 1 cm×2 cm, sheet resistance<15 Ω) by a BiOI template method. First of all, 5 mM $Bi(NO_3)_3·5H_2O$ (99.0%, Aladdin) and 5 mM KI (99.0%, Sigma-Aldrich) aqueous solution were used as the Bi^{3+} and I^- precursor solution, respectively. Next, a piece of FTO was vertically immersed into the Bi^{3+} precursor solution for 10 s, and then into the I^- precursor solution for 10 s. This immersion operation was repeated for 10 min to form an orange-red BiOI layer on the FTO. Then, 100 μL of 0.2 M $VO(acac)_2$ (99.5%, Aladdin) dimethyl sulfoxide solution was dripped on the BiOI layer, and annealed in air at 450℃ for 120 min. Finally, the resultant $BiVO_4$ film with excess vanadium oxide on surface was soaked into 2 M KOH for 30 min with gentle stirring to remove the vanadium oxide. For comparison, the as-prepared $BiVO_4$ film was further post-annealed in argon-saturated environment at 400℃ for 2 h.

1.2 Preparation of $Cu_3Mo_2O_9/BiVO_4$ film

The $Cu_3Mo_2O_9/BiVO_4$ film was prepared by hydrothermal approach with post-annealing. The experimental procedures are as follows. (1) 2.25 mM cupric nitrate $Cu(NO_3)_2$, 99.99%) and sodium molybdate dihydrate ($Na_2MoO_4·2H_2O$, 99.995%) aqueous solution was used as the precursor solution. (2) 30 mL of Cu^{2+}/Mo^{6+} precursor solution was transferred into a Teflon-lined autoclave (50 mL), and the as-prepared $BiVO_4$ film was vertically put into the precursor solution. (3) The Teflon-lined autoclave was kept at 180 °C for 15 h of hydrothermal reaction. (4) After the hydrothermal reaction, the resultant film was annealed in argon-saturated environment at 400℃ for 2 h. In addition, $CuOx/BiVO_4$ film was prepared for comparison to the $Cu_3Mo_2O_9/BiVO_4$ film. The CuOx nanoparticles are the mixture of Cu_2O and CuO nanoparticles that were synthesized by a hydrothermal reaction at 160℃ for 8 h using 0.1 M cupric acetate aqueous solution. After the hydrothermal reaction, 30 μL of hydrothermal reaction solution that contains CuOx nanoparticles was dripped on the $BiVO_4$ film. The resultant film was dried at 60℃ for 1 h, and then annealed at 400℃ for 2 h in air. The XRD characterization of the CuOx nanoparticles and

the preparation optimization for the CuOx/$BiVO_4$ film were shown in **Figure S1.**

For comparison, $Cu_3Mo_2O_9$ film was prepared through coating $Cu_3Mo_2O_9$ nanoparticles on the FTO. Specifically, after the hydrothermal reaction for the preparation of $Cu_3Mo_2O_9$/$BiVO_4$ film, 50 μL of hydrothermal reaction solution that contains $Cu_3Mo_2O_9$ nanoparticles was dripped on the FTO, and then be dried at 80℃ for 1 h. Finally, the $Cu_3Mo_2O_9$ nanoparticles-coupled FTO was annealed at 400℃ for 2 h in argon-saturated environment.

1.3 Material characterizations

The morphology and elemental composition of $BiVO_4$, $Cu_3Mo_2O_9$ and $Cu_3Mo_2O_9$/$BiVO_4$ films were investigated using a scanning electron microscope with EDS mapping function (SEM, Zeiss Supra 55 VP). The crystal phase of the as-prepared samples was checked by X-ray diffractometer (XRD, PANalytical X'pert PRO diffractometer). X-ray photoelectron spectroscopy (XPS) investigations for the samples were performed on a Kratos AXIS Ultra DLD XPS system. The UV-Vis absorption and photoluminescence (PL) emission spectra of the films were recorded on a Shimadzu UV-2600/2700 spectrophotometer and a SPEX 500 M spectrometer (in air at 25℃, 325 nm laser as the excitation source), respectively. In addition, the films were analyzed by laser Raman spectrometer (Renishaw inVia Raman). After 5 h of stability testing, the dissolved V and Bi from the $BiVO_4$ and $Cu_3Mo_2O_9$/$BiVO_4$ film photoanodes into the NaPi electrolyte were detected by inductively coupled plasma atomic emission spectrometry (ICP-AES, Thermo ICAP6300).

1.4 Electrochemical and photoelectrochemical measurements

The electrochemical and photoelectrochemical measurements for the film samples were carried out on CHI660E workstation with a three-electrode system. A Pt wire electrode and a saturated calomel electrode (SCE) were used as the counter electrode and reference electrode, respectively. 0.2 M NaPi buffer solution (Na_2HPO_4/NaH_2PO_4, pH 6.8) was used as the electrolyte. For the PEC measurements, a 300W xenon lamp with an AM 1.5G filter (Beijing China Education Au-light *Co. Ltd.*) was used to provide 100 mW/cm^2 simulated sunlight irradiation. The PEC measurements were performed using backside irradiation, namely, the irradiation passed through the FTO and then

reached on the film. The measured potentials *vs.* SCE reference electrode were converted into the potentials *vs.* reversible hydrogen reference electrode (RHE) though the following Nernst equation.

$$E_{RHE}=E^{\theta}_{SCE}+E_{SCE}+0.059pH \quad (E^{\theta}_{SCE}=0.2415 \text{ V } vs. \text{ NHE, at 298K}) \qquad (S1)$$

The electrochemically active surface area (ECSA) of the $BiVO_4$ and $Cu_3Mo_2O_9/BiVO_4$ film was measured and calculated by equation (2).

$$ECSA= C_{dl}/C_S \qquad (S2)$$

Where C_{dl} is the double-layer capacitance of the film electrode, C_s is the specific capacitance of the FTO electrode. C_{dl} was measured by cyclic voltammograms (CVs) in a non-Faradaic range from 0.75 to 0.95 V *vs.* RHE with different scan rates (shown in **Figure S5b** and **S5c**). The anodic-cathodic current density (ΔI) at 0.85 V *vs.* RHE, and the scan rate extracted from a series of CV curves were fitted into a linear relationship (**Figure S5e**), and the value of C_{dl} was the half of the slope of ΔI *vs.* scan rates curve. Since the surface of $BiVO_4$-based film electrodes are not smooth as expected, the C_s value of the $BiVO_4$-based film electrodes was placed by the C_s of the FTO electrode to calculate their ECSA.

The incident photon-to-current conversion efficiency (IPCE) for the film photoanodes was measured at 1.23 V *vs.* RHE in 0.2 M NaPi buffer under monochromatic light of 400-530nm irradiation. The equation (3) was used to calculate the films' IPCE.

$$IPCE(\%) = (1240 \times j) / (P_{light} \times \lambda) \times 100\% \qquad (S3)$$

Where j is the photocurrent density of film (mA/cm^2) under monochromatic light irradiation, P_{light} is the power density of incident light (mW/cm^2), and λ represents the wavelength of incident light (nm).

The Faradaic efficiency of the $Cu_3Mo_2O_9/BiVO_4$ film photoanode for O_2 evolution reaction was checked. Under AM 1.5 G illumination, the $Cu_3Mo_2O_9/BiVO_4$ photoanode was put into a gas-tight cell that linked with an Agilent 7890B gas chromatography. The amount of O_2 evolution on the photoanode at 1.23 V *vs.* RHE was detected by the gas chromatography, and the photogenerated charge was recorded on a CHI660E workstation. The Faradaic

efficiency of O_2 evolution [$\eta(O_2)$] on the $Cu_3Mo_2O_9/BiVO_4$ photoanode was calculated with the following equation.

$$\eta(O_2) = (\text{detected } O_2 \text{ evolution amount}) \times 100/(\text{theoretical } O_2 \text{ evolution}) \qquad (S4)$$

The intensity modulated photocurrent spectroscopy (IMPS) for the film photoanodes was measured to investigate their charge transfer property. The IMPS and IMVS measurements were performed on a Zennium PP211 station with the frequency of 100 K to 0.1 Hz, and 365 nm monochromatic light with a power density of 100 mW/cm^2 was used as the irradiation source. The average holes-transfer time (τ) of the film photoanodes was estimated by the following equation.

$$\tau_{tr} = 1 / (2\pi f_{min}) \qquad (S5)$$

where the f_{min} is the minimum frequency in the imaginary components of IMPS or IMVS.

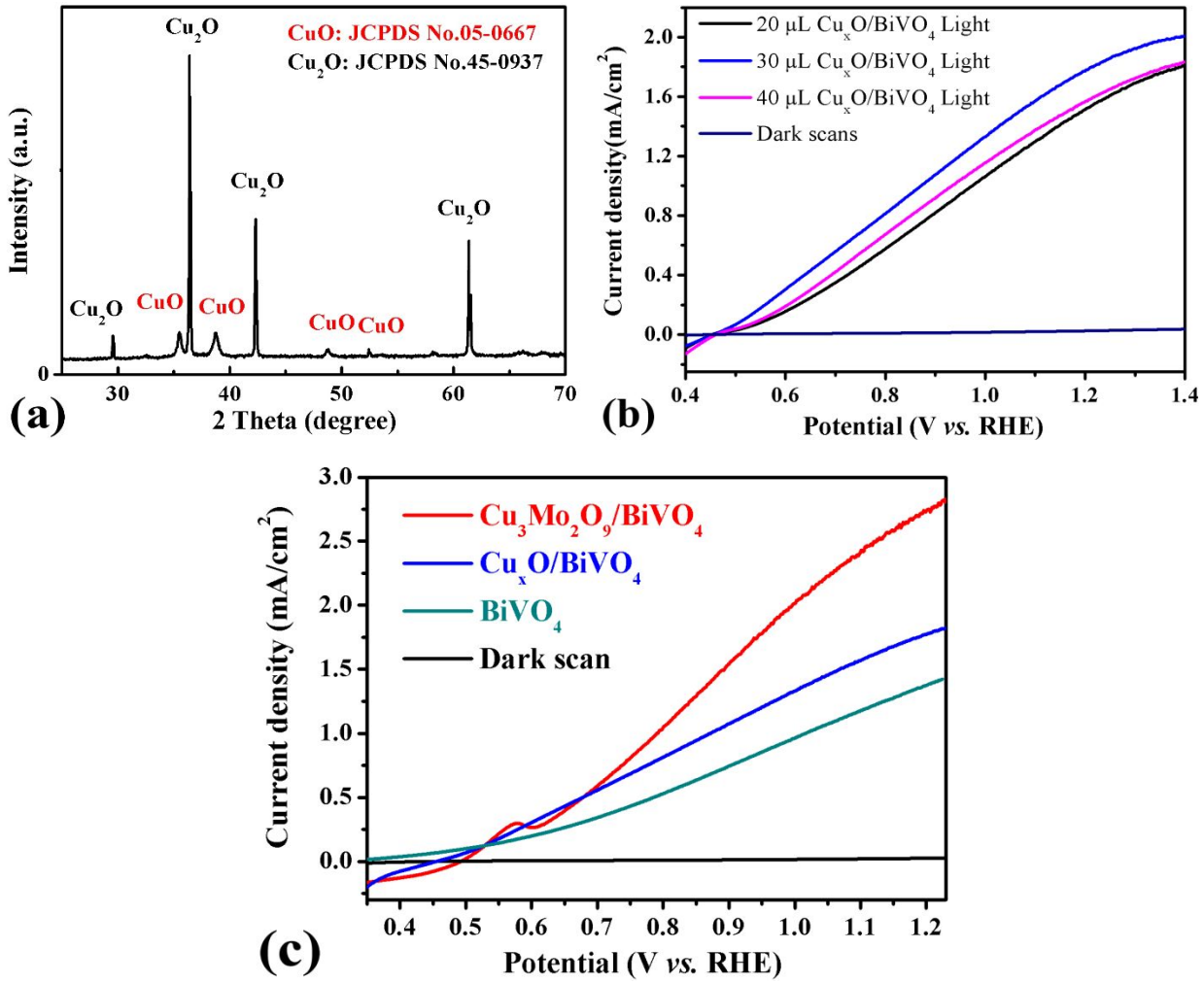

Figure S1. (a) XRD pattern of the as-prepared copper oxides sample. (b) LSV scans for the copper oxides/$BiVO_4$ films that prepared by coupling different amount of copper oxides. (c) LSV scans for the optimized copper oxides/$BiVO_4$ film and the $Cu_3Mo_2O_9/BiVO_4$ film. The LSV scan conducted in 0.2 M NaPi buffer under AM 1.5G illumination with a scan rate of 15 mV/s.

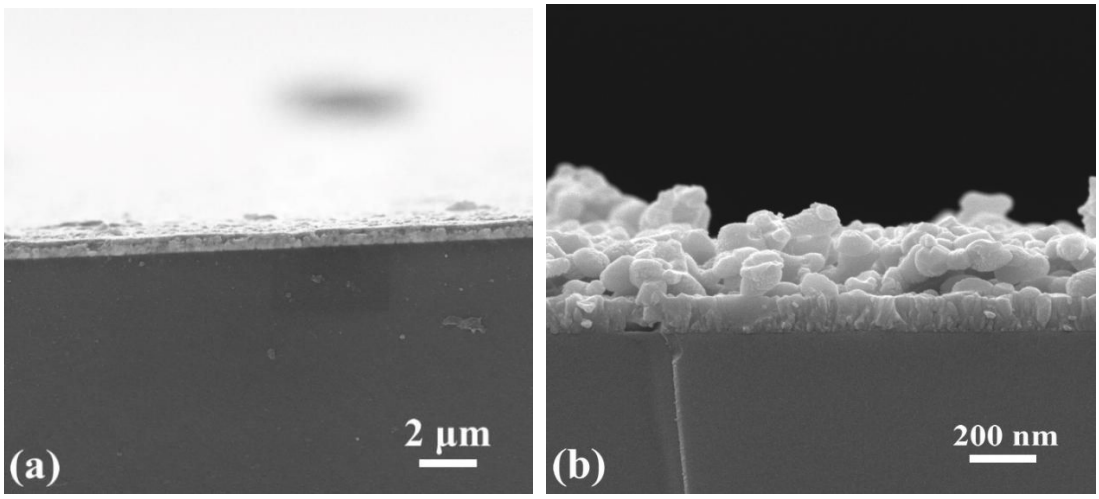

Figure S2. The cross-sectional SEM images (a) and (b) of the $Cu_3Mo_2O_9/BiVO_4$ film.

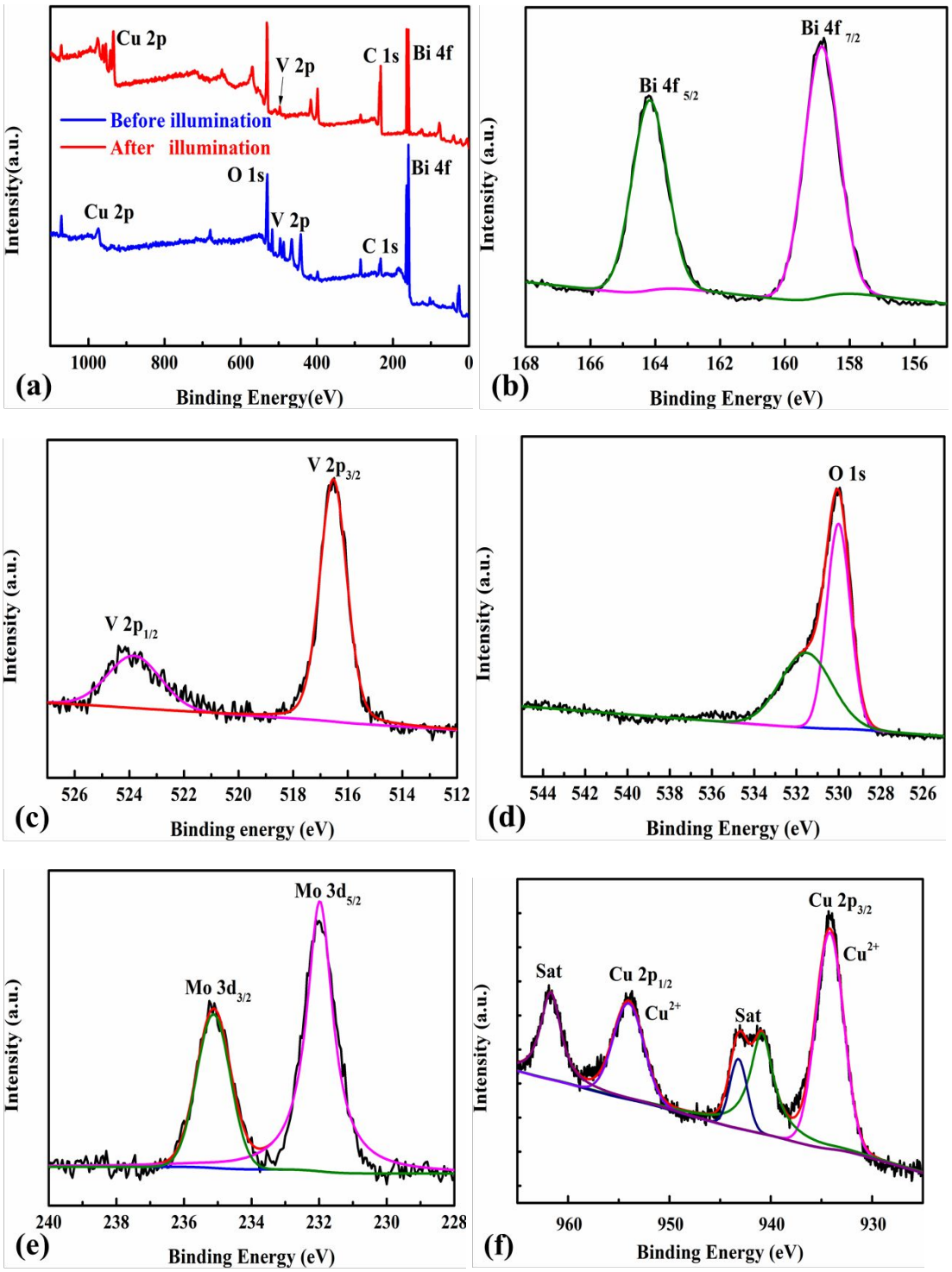

Figure S3. (a) Survey XPS spectrum of the $Cu_3Mo_2O_9/BiVO_4$ film. High-resolution (b) Bi 4f, (c) V 2p, (d) O 1s, (e) Mo 3d and (f) Cu 2p XPS spectrum of the $Cu_3Mo_2O_9/BiVO_4$ film.

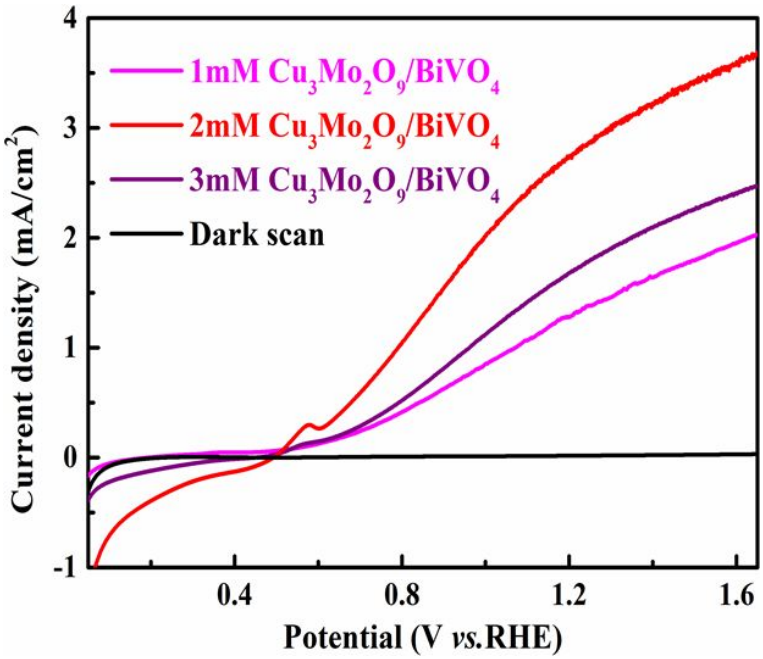

Figure S4. LSV scans for the $Cu_3Mo_2O_9/BiVO_4$ films that be prepared using different Cu^{2+}, Mo^{6+}-concentrations of precursor solution under same hydrothermal temperature and time.

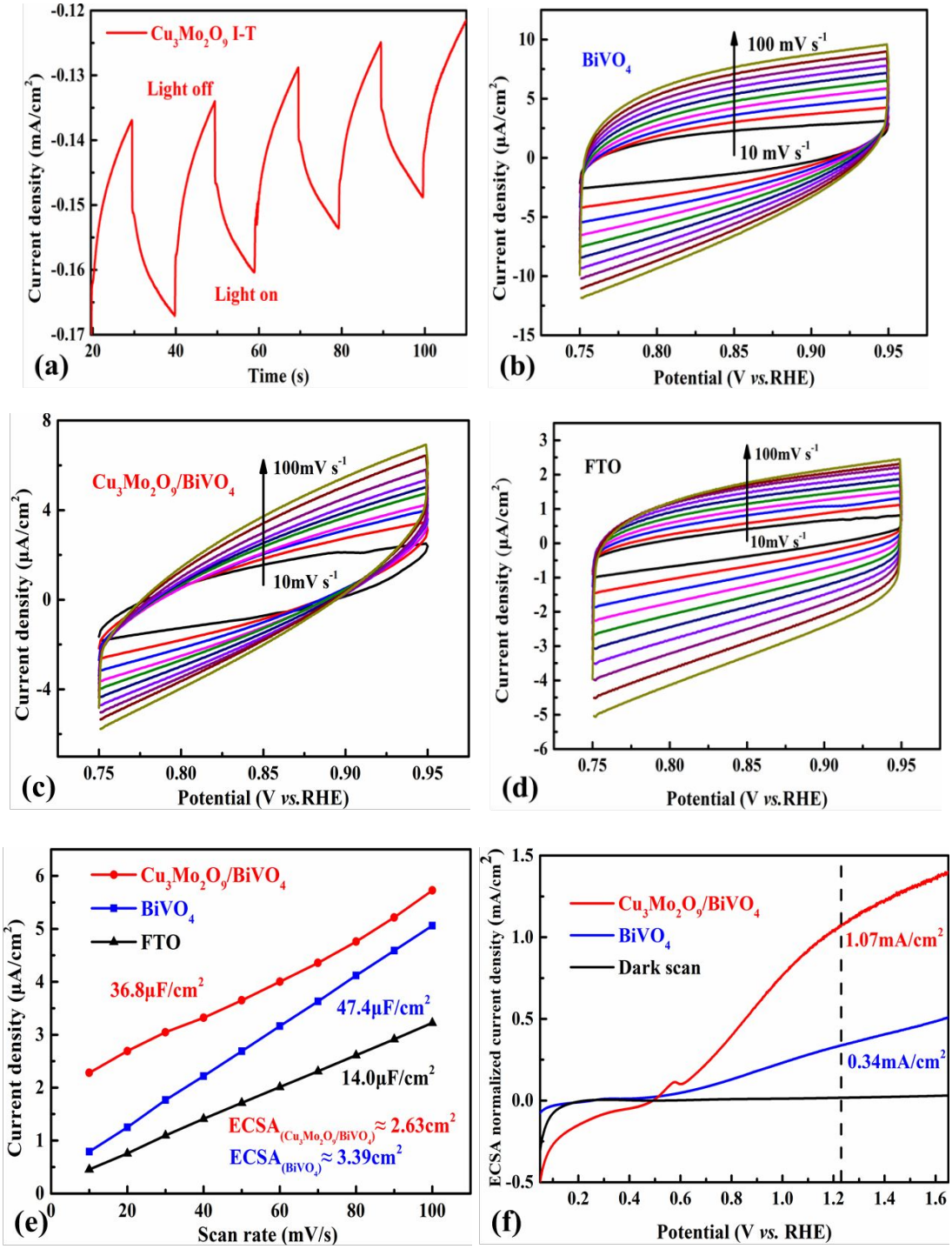

Figure S5. (a) *j-t* curve of the $Cu_3Mo_2O_9$ film at 0.1 V *vs.* RHE in 0.2 M NaPi under chopped AM 1.5 G illumination. CV curves of the (b) bare $BiVO_4$, (c) $Cu_3Mo_2O_9/BiVO_4$ film and (d) FTO in 0.2 M NaPi with scan rates of 10, 20, 30, 40, 50, 60, 70, 80, 90 and 100 mV/s. (e) The $\Delta I \sim v$ plots used for the determination of double-layer capacitance (C_{dl}) at 0.85V *vs*. RHE for the bare $BiVO_4$ and $Cu_3Mo_2O_9/BiVO_4$ film. (f) The ECSA normalized photocurrent density vs. voltage curves for the bare $BiVO_4$ and $Cu_3Mo_2O_9/BiVO_4$ film in 0.2 M NaPi.

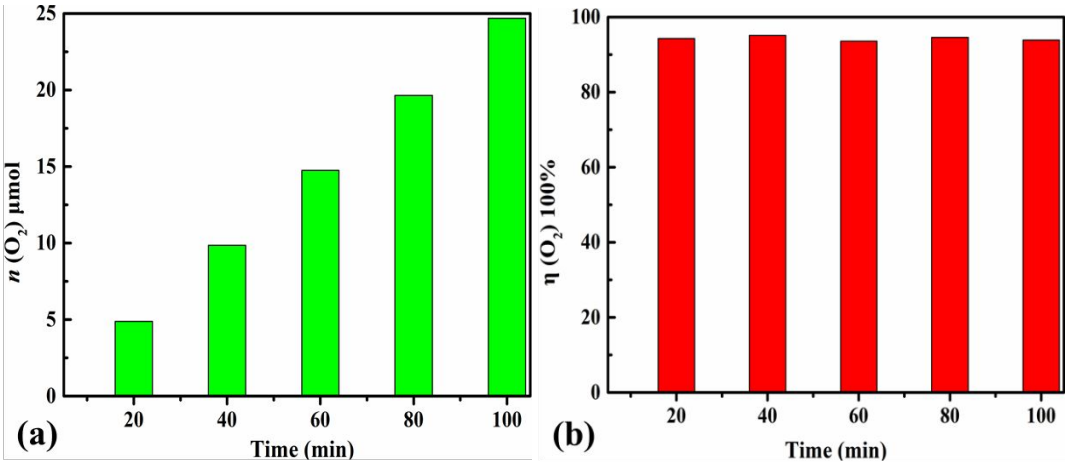

Figure S6. (a) The O_2 generation amount and (b) Faradaic efficiency for the $Cu_3Mo_2O_9/BiVO_4$ film in 0.2 M NaPi under AM 1.5G illumination.

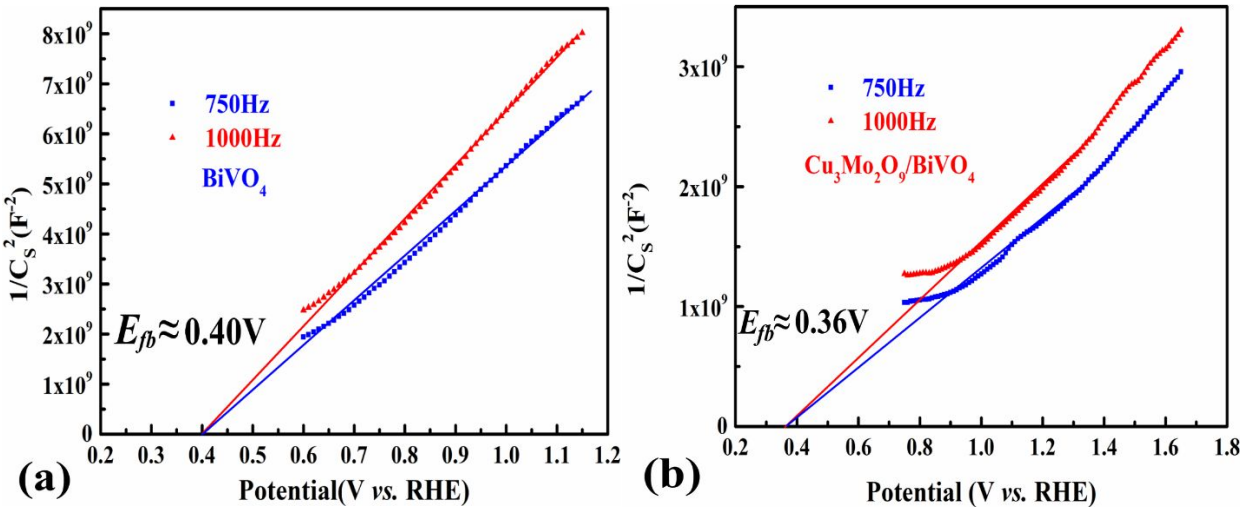

Figure S7. Mott-Schottky plots of (a) the bare $BiVO_4$ and (b) $Cu_3Mo_2O_9/BiVO_4$ film photoanode in 0.2M NaPi buffer.

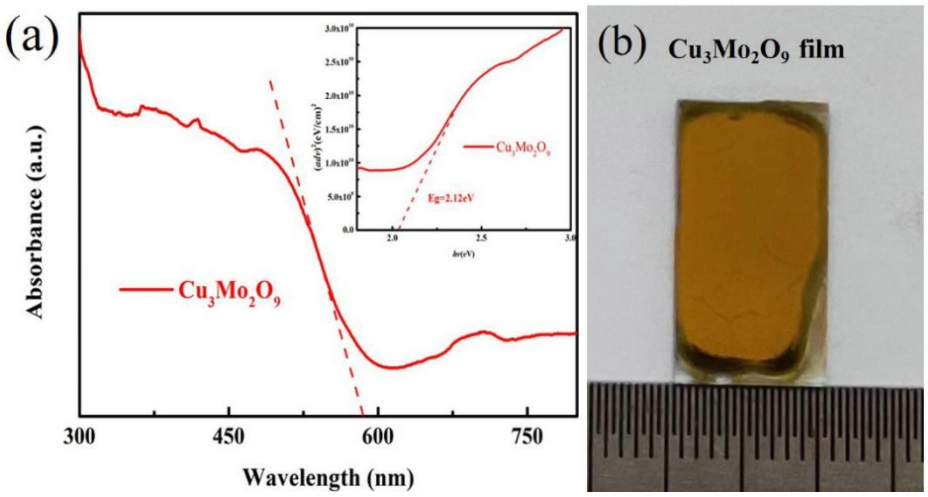

Figure S8. (a) UV-Vis absorbance spectrum and the related Tauc plots of the as-prepared $Cu_3Mo_2O_9$ powder. (b) The photograph of the as-prepared $Cu_3Mo_2O_9$ film.

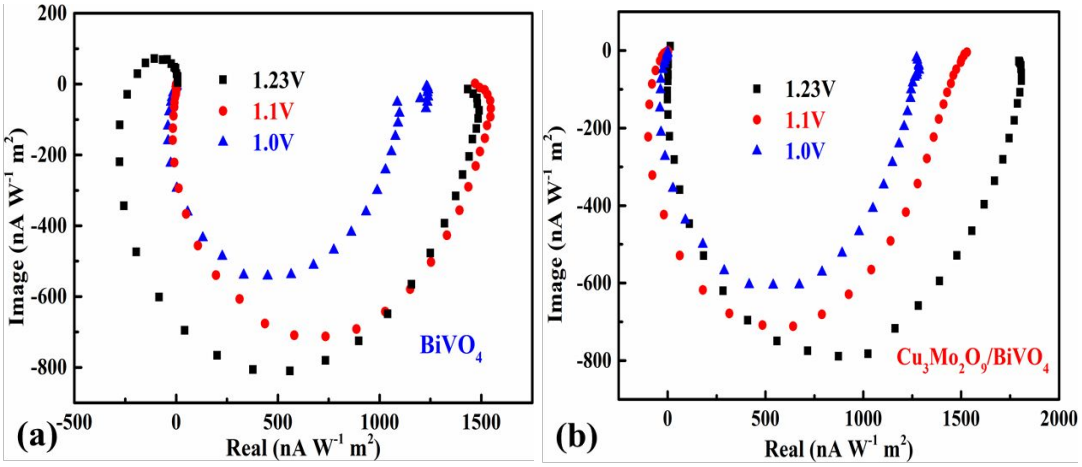

Figure S9. IMPS plots of the (a) bare $BiVO_4$ film photoanode and (b) $Cu_3Mo_2O_9/BiVO_4$ film photoanode in 0.2 M NaPi buffer (pH6.8) under an incident light wavelength of 365 nm (100 mW/cm^2) at 1.0, 1.1, 1.23V *vs.* RHE, respectively.

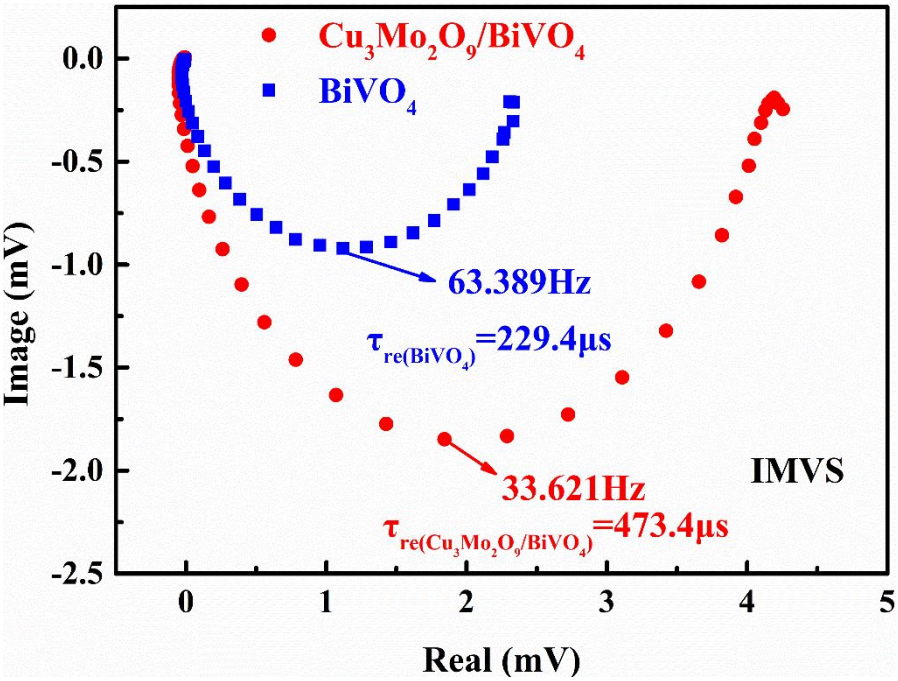

Figure S10. The IMVS plots and surface charge recombination time (τ_{re}) of the bare $BiVO_4$ and $Cu_3Mo_2O_9/BiVO_4$ film photoanode at 1.23 V *vs.* RHE in 0.2 M NaPi buffer.

Table S1 The fitted element value for the equivalent circuit shown in the Nyquist Plots for the bare $BiVO_4$ (**Figure 5c**) and $Cu_3Mo_2O_9/BiVO_4$ film photoanode (**Figure 5d**).

Sample	Rs/Ω (error/%)	CPE/F (error/%)	Rct/Ω (error/%)
$BiVO_4$	38.04 (1.16%)	8.182E-5 (5.89%)	509.3 (1.24%)

Sample	Rs/Ω (error/%)	CPE_1/F (error/%)	Rct_1/Ω (error/%)	CPE_2/F (error/%)	Rct_2/Ω (error/%)
$Cu_3Mo_2O_9/BiVO_4$	35.82 (1.42%)	1.374E-5 (9.09%)	47.8 (9.61%)	2.028E-5 (7.68%)	130.6 (7.49%)